IX International Conference on Computational Methods for Coupled Problems in Science and Engineering
COUPLED PROBLEMS 2021
E. Oñate, M. Papadrakakis and B. Schrefler (Eds)

SIMULATION OF TALL-3D EXPERIMENTAL FACILITY WITH A MULTISCALE AND MULTIPHYSICS COMPUTATIONAL PLATFORM

Giacomo Barbi[1*], Antonio Cervone[2], Andrea Chierici[1], Leonardo Chirco[3], Roberto Da Vià[4], Federico Franceschini[1], Valentina Giovacchini[1] and Sandro Manservisi[1]

[1]University of Bologna, DIN, Lab. of Montecuccolino, Via dei Colli 16, Bologna 40136, Italy
[2]Italian National Agency for New Technologies, Energy and Sustainable Economic Development, ENEA, Via Martiri di Monte Sole 4, Bologna 40129, Italy
[3] Sorbonne Universit, Institut Jean Le Rond d'Alembert, 4 Place Jussieu, Paris, France
[4] SuperComputing Applications and Innovation Department-CINECA, Bologna 40033, Italy
[*] e-mail: giacomo.barbi3@unibo.it

Key words: Coupled Problems, Multiphysics Problems, TALL-3D, LFR technology

Abstract. This work details the development of a computational platform in joint collaboration between the Italian National Agency for New Technologies, Energy and Sustainable Economic Development (ENEA) and the University of Bologna (UNIBO). The platform is based on the open-source SALOME software that integrates the CATHARE system code for nuclear safety, FEMUS and OpenFOAM CFD codes in a unique framework, with efficient methods for data exchange.

The computational platform has been used to simulate complex multiscale and multiphysics systems, such as the TALL-3D facility, with a defective boundary condition approach on overlapping domains. The TALL-3D experimental facility has been realized with the purpose of providing reference results to be used for both standalone and coupled System Thermal-Hydraulic (STH) and Computational Fluid Dynamic (CFD) code validation. The transient phenomenon of unprotected loss of lead-bismuth eutectic (LBE) flow that has been experimentally simulated at TALL-3D is here studied. The system code is used to simulate the TALL-3D apparatus while the CFD code is used to get a better insight into the fluid streaming occurring in the main tank component and improve the system code predictions. A flow transition from forced to natural convection is used to validate the codes and the platform ability to reproduce the experimental data.

1 Introduction

Nowadays, the rapidly increasing computational power allows scientists and engineers to use computational tools in the design process of complex systems. Many numerical

codes are available, from both the commercial and open-source sides, and can be used for simulating a very wide set of physical phenomena. A further step in the numerical simulation process is represented by the numerical code coupling procedure. This strategy can be used when a very complex system has to be studied, where several physical phenomena interact on a wide range of physical scales. The realization of a huge numerical code capable of simulating all the physical phenomena of interest is then avoided and the effort is put on the design of an environment where numerical codes can be run independently with appropriate exchange data. Following this idea, a joint collaboration between the Italian National Agency for New Technologies, Energy and Sustainable Economic Development (ENEA) and the University of Bologna (UNIBO) led to the development of a computational platform. This platform integrates OpenFOAM and FEMuS, open-source finite volume and finite element codes, respectively, for Computational Fluid Dynamic (CFD) simulations, and the system code CATHARE [1, 2, 3].

These codes allow performing multi-scale simulations of complex systems such as experimental apparatus or, as a final aim, sections of a nuclear power plant. For these systems, a CFD simulation of the full system would be too expensive in terms of computational cost, while a system code is not sufficient to tackle complex transient situations. With the coupled simulations a better insight into the phenomena occurring in some components can be obtained by simulating them with a CFD code and using the obtained results to improve the system code simulation. The numeric platform has been used to perform simulations of the evolution of an unprotected loss of flow going from forced to natural circulation flow in the experimental TALL-3D facility. TALL-3D is a liquid Lead Bismuth Eutectic loop with an oil-cooled secondary loop, developed at KTH (Royal Institute of Technology, Stockholm, Sweden) as part of the EU THINS project. It was designed in order to provide mutual feedback between natural circulation in the loop and complex 3D mixing and stratification phenomena in a pool-type test section, and to give the possibility to validate the standalone system and CFD codes for each subsection of the facility [4].

This paper summarizes the results obtained from the joint collaboration between ENEA and UNIBO, showing the consistency of the developed algorithm for multi-scale simulations, with the intent to provide a suitable tool for studying issues of LFR technology. The coupling between FEMuS-OpenFOAM CFD codes and CATHARE system code is based on an overlapping domain method [5, 6, 7]. In the first part, the main attention is put on CFD analysis of the test section where further boundary conditions are tested to achieve more accurate simulation results. Then, the code coupling between CATHARE and OpenFOAM will be performed. The results of the coupled numerical simulation are compared with the experimental results, in order to validate the codes and the presented coupling algorithm for nuclear power safety analysis.

2 Numerical Modeling

The TALL-3D facility modeled with the system code CATHARE is summarized in Figure 1. We can notice a primary loop with the sump tank to store, melt and supply lead-bismuth into the main loop, three vertical legs (named Main Heater, 3D and Heat Exchanger leg) and two connecting horizontal sections each combining two elbows and a T-junction. CFD simulations are performed in the 3D test section connected by the 3D leg, while a secondary loop with Dowtherm RP is used as heat transfer fluid to control the heat balance in the primary loop. Further information are available in the following references [4, 8].

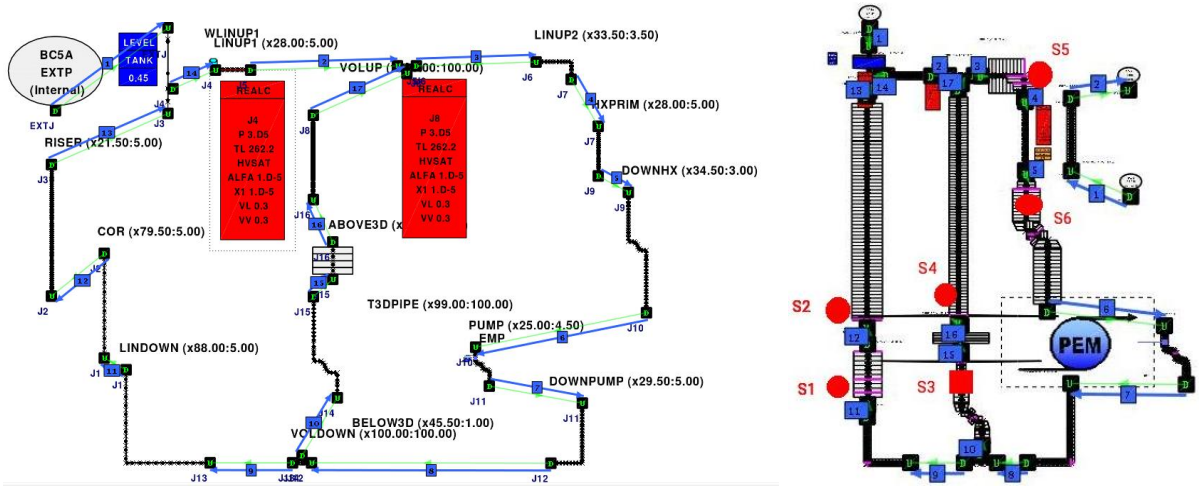

Figure 1: CATHARE model for the TALL-3D facility (left) and points of interest (right) S1-S2 of the Main Heater leg, S3-S4 of the 3D leg and S5-S6 of the Heat Exchanger leg.

In this work, the platform SALOME is used with the aim to link and couple the different codes [8]. The data transfer has been realized through the use of the MEDMem library, and a SALOME interface has been built in the system code CATHARE. The coupling is obtained by duplicating the mesh of the CFD code in the MED format, and projecting the solution fields on it. Then, implemented functions allow to project or integrate all the variables on a desired portion of the MED interface, and to project the obtained values in the target code. Concerning the dimensional mesh, a 1D-domain has been adopted for the system code meanwhile, a 3D domain has been used to model the test section with the CFD code. The latter is completed with the boundary conditions coming from the solutions of the corresponding field on the CATHARE code. Moreover, a defective method is used to give feedback information from CFD code to system code.

2.1 Developed boundary conditions in OpenFOAM

In this work, a k-ω turbulence model is used to solve the momentum equation for the 3D region with the CFD code. Additional boundary conditions have been implemented

in OpenFOAM to take into account the heat exchange between TALL-3D apparatus and the surrounding environment, but also between the fluid and the steel disk that is located inside TALL-3D geometry. The influence of these boundary conditions has been evaluated by using experimental data as inlet boundary conditions, for the CFD simulation, instead of the coupling with CATHARE code. This procedure allows evaluating the effect of the new modeled phenomena on the CFD solution without the influence of the system code. The boundary conditions have been implemented as new code classes within OpenFOAM. The usage of each class is explained in the next paragraph.

A sketch of the simulated geometry is shown in Figure 2 a). Labels for the boundaries on inlet-outlet sections (Γ_i and Γ_o) and inlet-outlet channels ($\Gamma_{w,ch,i}$ and $\Gamma_{w,ch,o}$) are shown in Figure 2 a). On Figure 2 b) boundary labels, on a close up view of the test section, define the heated surface Γ_h, the fluid-disk interface Γ_d, the bottom, the side and top test section walls ($\Gamma_{w,b}$, $\Gamma_{w,s}$ and $\Gamma_{w,t}$).

Heat exchange with surrounding environment The presence of a non neglectable heat exchange between TALL-3D apparatus and the surrounding environment can be inferred from a simple energy balance. Before the pressure drop, in steady condition, the following experimental data are read: mass flow rate $\dot{m} \simeq 1.9\ kg/s$ and outlet-inlet temperature difference $\Delta T \simeq 35°C$. We consider constant physical properties calculated at reference temperature $T_{ref} = 272.5°C$, leading to a specific heat capacity value $c_p = 147\ J/kgK$. These values lead to a heat flux q, applied on the heated area, equal to 88505 W/m^2, while the imposed one is 99900 W/m^2. A thermal power $Q_d \simeq 1100\ W$ is

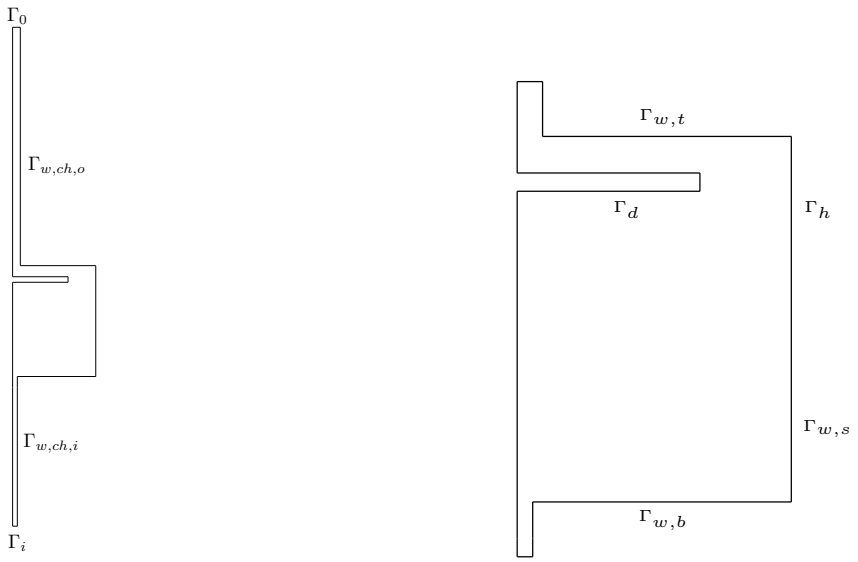

Figure 2: Radial section of the TALL-3D apparatus showing the surrounding environment between fluid and steel disk (a) with close up view of the test section (b). Boundary labels are shown.

then exchanged with surrounding environment. The boundary condition is modeled as non-constant and non-uniform heat flux applied q_d on selected wall boundaries. Heat flux q_d is modeled as

$$q_d = \frac{Q_d}{A_d} = h_{ex}(T_w - T_{env})\,, \tag{1}$$

where A_d is the area of the wall, h_{ex} the heat exchange coefficient, T_w the wall temperature and T_{env} the environment temperature. A uniform value of h_{ex} is estimated from a preliminary steady CFD calculation with the following settings:

- heat flux $q = 88505\ W/m^2$ applied on the heated area;
- no heat exchange with the environment;
- temperature T_w calculated as mean integral temperature value of the wall boundaries where heat exchange with the environment will be considered;
- constant environment temperature $T_{env} = 25°C$.

In order to use this boundary condition, the condition needs to be set in the relative OpenFOAM temperature field file.

Heat exchange with immersed steel disk A simplified model for the heat exchange with the immersed steel disk has been considered. In particular, the disk temperature is considered to be uniform, providing a great simplification in modeling the new boundary condition. The following energy balance for the solid disk holds

$$dm\ c_p\ \Delta T = \dot{q}\ dA\ \Delta t\,. \tag{2}$$

Equation (2) refers to the temperature variation ΔT of solid mass dm due to the presence of heat flux $\dot{q}$ applied on surface dA for a time interval Δt. Since the disk temperature is considered to be uniform, equation (2) can be integrated over the entire disk volume, leading to the following discrete form

$$m\ c_p\ \Delta T = \sum_i \dot{q}_i A_i\ \Delta t\,, \tag{3}$$

where $\dot{q}_i$ and A_i refer to the heat flux and the surface of i-th boundary element. At each time step the solid temperature is calculated as

$$T^{new} = T^{old} + \frac{\sum_i \dot{q}_i^{old} A_i\ \Delta t}{m\ c_p}\,. \tag{4}$$

The boundary condition is then implemented as a nonuniform heat flux $\dot{q}$ imposed on the boundary surface that represents the fluid-disk interface. With the new calculated disk

temperature, for each cell having a face on fluid-disk interface the heat flux is calculated as

$$\dot{q}_i = -k\frac{T_i - T^{new}}{h_i}\,, \tag{5}$$

where T_i is the cell temperature value and h_i is the cell center to boundary face distance.

2.2 Coupling algorithm - Defective method

Considering a generic variable of CATHARE φ, which is improved by the solution of the CFD simulation, we can define respectively φ_{1D} and φ_{CFD} calculated as a mean integral value. The method relies on the introduction of a fictitious source term $\mathcal{S}^n$, written using the value at the previous time step as

$$\mathcal{S}^n = \mathcal{S}^{n-1} - \omega_\varphi(\varphi_{CFD} - \varphi_{1D})\,, \tag{6}$$

where ω_φ is an under relaxation parameter smaller than 1. This equation is iteratively solved, allowing to correct the system code solution φ_{1D} with the value of CFD solution φ_{CFD}, until they are equal.

From the right of Figure 1, different reference points in the TALL-3D system are considered ($S1$, $S2$, $S3$, $S4$, $S5$, $S6$), and particular attention is given to $S3$ and $S4$ points located before and after the 3D test section where the codes are coupled. More accurately, the point S3 is the 1D-3D matching interface for the physical variables at the inlet section of the 3D region, meanwhile the point S4 is the 3D-1D matching interface for the outlet section of the 3D region.

Thus, OpenFOAM-CATHARE coupling can be achieved with the following algorithm:

- Stabilization of the 1D Problem (CATHARE); stabilization of state and turbulent variables of the 3D CFD problem to CATHARE setup (OpenFOAM);
- For each time step:
  - Defective correction from 3D near the outlet of the TALL3D component and one-step solution for the 1D code for velocity, temperature and pressure fields;
  - Boundary conditions from 1D at the inlet section of 3D geometry and one step solution for the 3D code for physical variables.

In order to correct the energy equation, the enthalpy source $ENTLEXT$ can be computed inside the corresponding equation. It is possible to define

$$ENTLEXT = h_{S4} - \alpha C_p(T_{1D} - T_{3D})\,, \tag{7}$$

where α is a constant and h_{S4}, T_{S4} are the enthalpy and the temperature at point S4, respectively. At the outlet of the 3D test section, we can define the T_{3D}, which is calculated at each time step by OpenFOAM. After that, it is possible to impose this temperature

value inside the STH code. At the same time, the momentum correction can be obtained by solving $DPLEXT$ as

$$DPLEXT = DPLXT_o - \beta(\Delta p_{3D} - \Delta p_{1D}) \,, \tag{8}$$

where β is a constant value and Δp_{3D} and Δp_{1D} are the pressure losses without the gravity contribution. From the STH code we can obtain the value of $DPLXT_o$ which is the old value of $DPLXT$.

3 Results

3.1 Results obtained with the new OpenFOAM boundary conditions

In the present section, results are discussed to evaluate the effect of heat exchange between TALL-3D apparatus and both surrounding environment and steel disk. This preliminary study can help to understand how the CFD simulation results can be improved. Moreover, improved CFD predictions will lead to improved results of the coupled CATHARE-OpenFOAM simulation, as it will be further investigated in the next subsection. Since heat exchange with the surrounding environment is here considered, a different geometry is investigated. In particular, the inlet and outlet sections are placed at the same locations where thermocouples TC2.1211 and TC2.2111 are installed in the experimental facility. For a better understanding of the new modelling hypothesis effects, the following cases are considered:

- case A: base case, adiabatic boundary conditions along solid boundaries and fluid-disk interface;
- case B: modelled heat exchange with surrounding environment on boundary $\Gamma_{w,ch,i}$;
- case C: same as case B with additional heat exchange on Γ_d;
- case D: heat dispersion on $\Gamma_{w,ch,o}$ and heat exchange on Γ_d;
- case E: same as case C with additional heat exchange on $\Gamma_{w,b}$, $\Gamma_{w,s}$ and $\Gamma_{w,t}$.

A comparison between experimental values and results obtained for case A are shown in Figure 3, where the heat flux $\dot{q}$ applied on the heated area is equal to $\dot{q} = 88505\, W/m^2$. In particular mean temperature difference between outlet and inlet sections are shown in Figure 3 a), while outlet temperature values are reported in Figure 3 b). It can be seen that outlet temperature values increase with time for $t > 20\, s$. After a rapid increase of temperature values, oscillations are observed, with peak values occurring at almost every 200 seconds from time $t \simeq 200\, s$. Results obtained for case A show a more intense temperature values increment followed by a long reduction. From time $t \simeq 500\, s$ temperature values slowly increase again. Temperature oscillations are slightly observed from Figure 3 b), while they are somehow depicted in Figure 3 a).

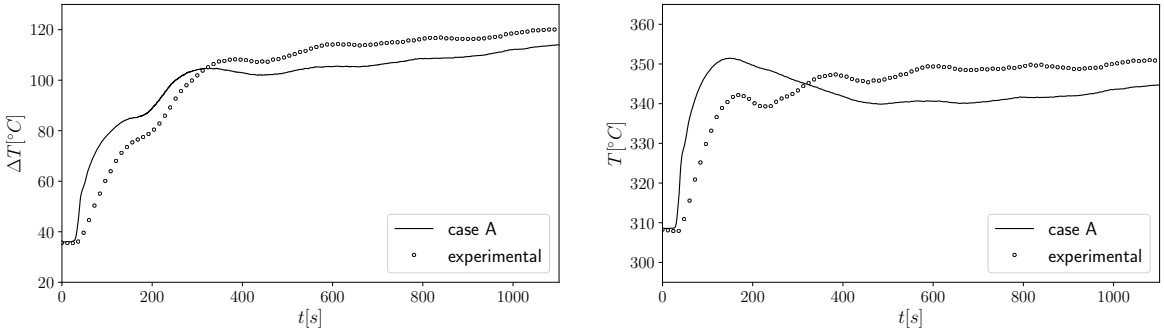

a) b)

Figure 3: Comparison between case A and experimental values of temperature difference between outlet and inlet section a) and outlet temperature values b).

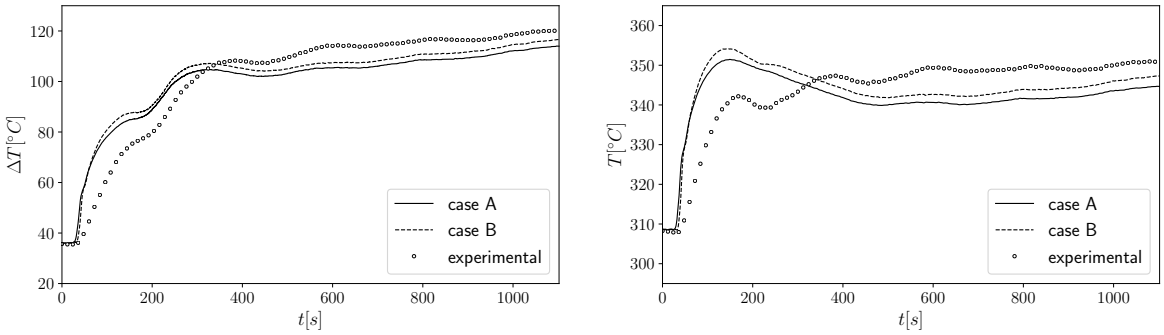

a) b)

Figure 4: Comparison between case A, case B and experimental values of temperature difference between outlet and inlet section a) and outlet temperature values b).

In case B heat exchange with the surrounding environment is taken into account. On the heated surface Γ_h the constant heat flux $\dot{q} = 99900\, W/m^2$ is imposed. Heat dispersion is considered distributed along the inlet channel external wall. Heat exchange coefficient h is evaluated following the procedure explained in Section 2.1. Comparisons between obtained results for cases A and B, with experimental data, for outlet-inlet temperature difference, and for outlet temperature values are shown in Figure 4 a) and b) respectively. It can be seen that the steady outlet temperature values overlap the experimental ones, showing that the heat transfer coefficient h, used to model the heat flux applied on boundary $\Gamma_{w,ch,in}$, has been correctly estimated. As a consequence of the greater heat flux value applied on the heated surface, higher temperature values are obtained during the transitory. For times $t > 300\, s$ obtained temperature values are slightly closer to experimental values but temperature fluctuations are not yet simulated.

Improved results have been obtained from the simulation of case C, as can be seen from the comparison of the outlet-inlet temperature difference and outlet temperature

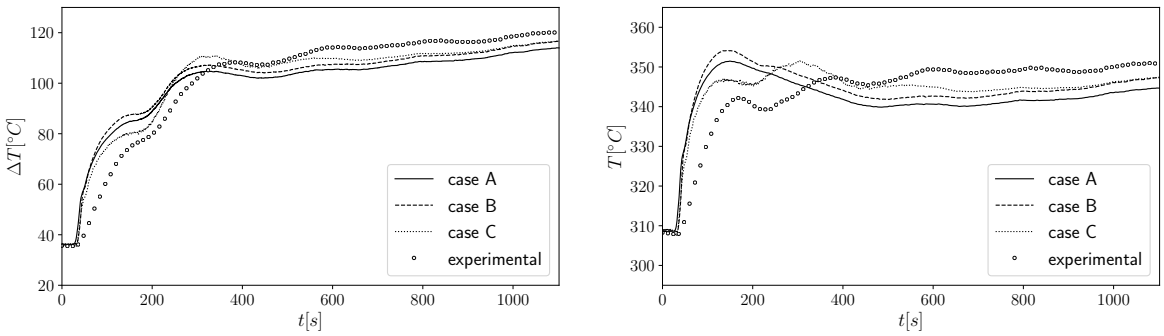

a) b)

Figure 5: Comparison between case A, B, C and experimental values of temperature difference between outlet and inlet section a) and outlet temperature values b).

values shown in Figure 5 a) and b) respectively. Heat exchange between the fluid and the steel disk introduces thermal inertia, reducing the outlet temperature peak value at $t \simeq 100\,s$. Differently from cases A and B, a second temperature peak value is observed at $t \simeq 300\,s$. It can be seen that the heat exchange with the disk has an influence in time interval $t \in [20; 900]\,s$ since for $t > 900\,s$ results obtained for case C overlap those obtained for case B.

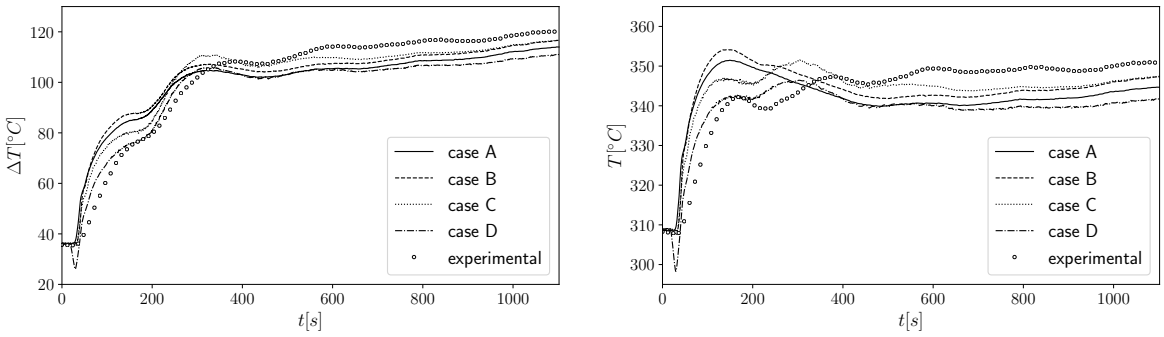

a) b)

Figure 6: Comparison between case A, B, C, D and experimental values of temperature difference between outlet and inlet section a) and outlet temperature values b).

A comparison of results for cases A, B, C, D and experimental data is reported in Figure 6 a) and b). It can be seen that if heat dispersion is distributed along boundary $\Gamma_{w,ch,o}$ then a sensible outlet temperature values decrease is obtained at the beginning of the transitory, with a phenomenon that is not observed from experimental values. Temperature oscillations are observed as in results of case C, but obtained values are in worst agreement with experimental data.

Having seen the importance of the heat exchange with the steel disk, even with a simplified model, as a final case, labeled as case E, we consider a heat exchange with

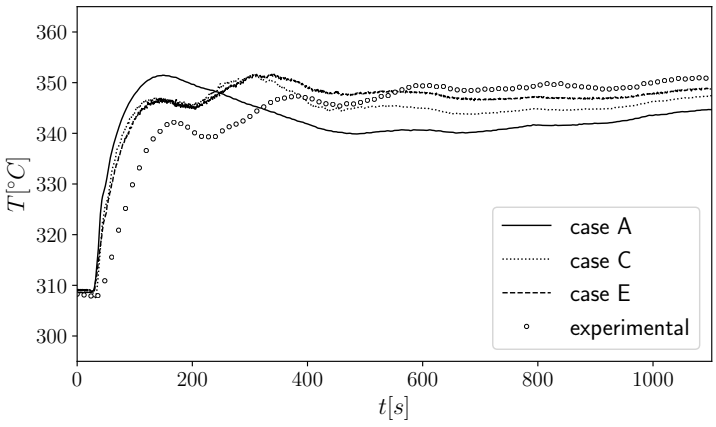

Figure 7: Comparison of outlet temperature values between cases A, C, E and experimental data.

the steel body of the test section, namely on boundaries $\Gamma_{w,b}$, $\Gamma_{w,s}$ and $\Gamma_{w,t}$. The three boundaries are considered as three different bodies, so each one has a different uniform temperature value. Time evolution of outlet temperature for cases A, C and E, together with experimental data, is shown in Figure 7. The presence of these additional heat exchanges has a slight influence at the beginning of the transitory while a more sensible effect is observed for $t > 300\,s$, where higher outlet temperature values are obtained, in particular with a better agreement with experimental data.

3.2 Results obtained with CATHARE-OpenFOAM coupling

In order to consider the overall behavior of the TALL-3D facility, the CATHARE-OpenFOAM coupling has been implemented. The last configuration, case E with the all heat dispersion, has been taken as a starting point for the code coupling. In Figure 8 the mass flow and the temperature fields are shown at the reference points given by the experimental data and the CATHARE-OpenFOAM coupling solution. At the top of Figure 8 we can notice the behavior at reference point S4, meanwhile at the bottom is shown the S3 reference point, both in the central leg. The experimental data are indicated through the experimental markers and the CATHARE-OpenFOAM coupling with the solid line. The inlet and outlet temperature decrease owing to the application of heat dispersion effects on the wall. This is needed when one requires to match experimental data. On the other hand, there are some discrepancies in the evaluation of the oscillation period and their amplitude.

4 Conclusions

In this paper, the experimental TALL-3D facility has been studied coupling the mono-dimensional solution of the system code CATHARE and the CFD solution obtained with OpenFOAM for the 3D domain (the test section). A natural circulation flow config-

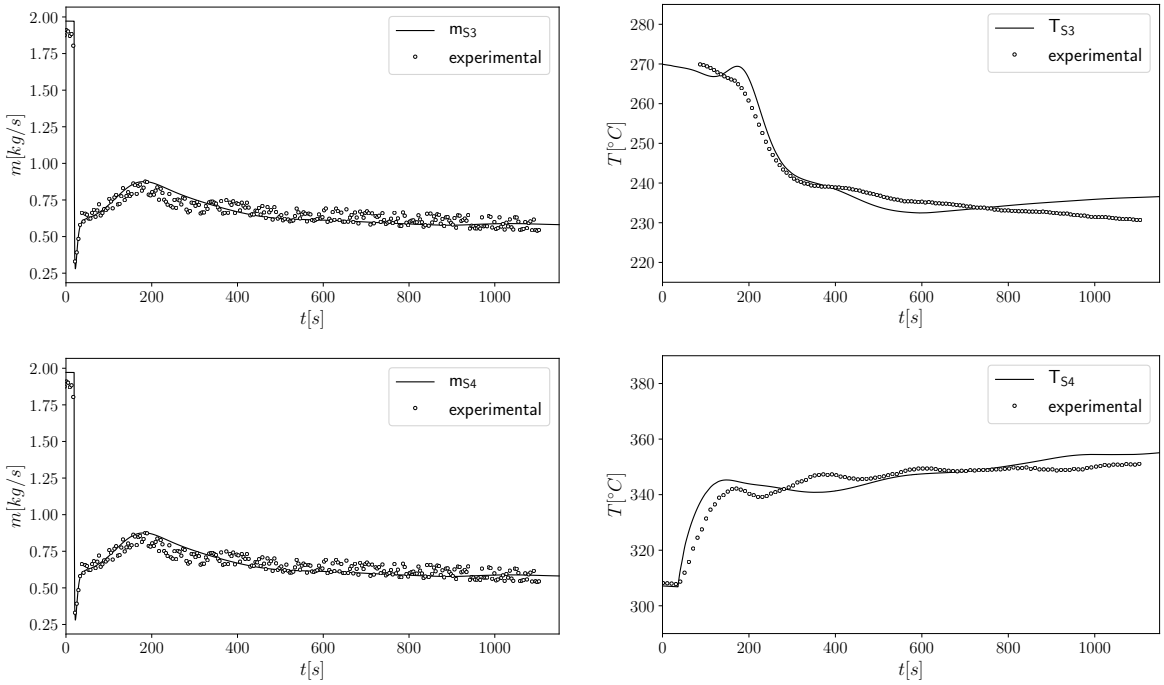

Figure 8: Mass flow rate (right) and temperature (left) at reference point S4 (top) and S3 (below) of the central leg for experimental data (∘) and coupling CATHARE-OpenFOAM with heat dispersion on the TALL-3D test section.

uration has been simulated with the aim of improving a multi-scale and multi-physics computational platform in order to design LFR technology.

This work has been developed through a strict collaboration between the University of Bologna and ENEA [9, 10, 11, 8, 12]. Further boundary conditions have been implemented in OpenFOAM taking into account the heat exchange between the TALL-3D main section and the external environment across the steel disk present inside the test section geometry. Experimental data have been taken as benchmark results to evaluate the accuracy of these boundary conditions for the CFD simulation, without the coupling with CATHARE code. A simple configuration with heat dispersion effect has been studied, and after that, the coupling with CATHARE has been implemented to consider the overall behavior of the TALL-3D facility. A good agreement has been shown after the code coupling, even though some discrepancies can be seen in different flow regimes. Further investigations will be required in order to achieve better simulation results both in the STH code and CFD modeling for LFR technology.

REFERENCES

[1] "https://www.openfoam.com/ - OpenFOAM project."

[2] "https://github.com/FemusPlatform/femus - Official repository for multigrid Finite

Element Code FEMuS ."

[3] D. Bestion, "The physical closure laws in the CATHARE code," *Nuclear Engineering and Design*, vol. 124, no. 3, pp. 229 – 245, 1990.

[4] D. Grishchenko, M. Jeltsov, K. Kööp, A. Karbojian, W. Villanueva, and P. Kudinov, "The TALL-3D facility design and commissioning tests for validation of coupled STH and CFD codes," *Nuclear Engineering and Design*, vol. 290, pp. 144 – 153, 2015.

[5] T. Grunloh and A. Manera, "A novel domain overlapping strategy for the multiscale coupling of CFD with 1D system codes with applications to transient flows," *Annals of Nuclear Energy*, vol. 90, pp. 422 – 432, 2016.

[6] R. Bavière, N. Tauveron, F. Perdu, E. Garrè, and S. Li, "A first system/CFD coupled simulation of a complete nuclear reactor transient using CATHARE2 and TRIO_U. Preliminary validation on the Phènix Reactor Natural Circulation Test," *Nuclear Engineering and Design*, vol. 277, p. 124137, 10 2014.

[7] A. Chierici, L. Chirco, R. Da Vià, S. Manservisi, and R. Scardovelli, "A multiscale numerical algorithm for heat transfer simulation between multidimensional cfd and monodimensional system codes," in *Journal of Physics: Conference Series*, vol. 923, p. 012025, IOP Publishing, 2017.

[8] A. Cervone, A. Chierici, L. Chirico, R. Vià, and S. Manservisi, "Validation of a multiscale coupling algorithm by experimental tests in tall-3D facility," in *6th ECCM and 7th ECFD ECCOMAS 2018 conference*, pp. 1605–1616, 2020.

[9] D. Cerroni, A. Cervone, R. Da Vià, and S. Manservisi, "Validation of the FEMLCORE-CATHARE coupling model of the TALL-3D facility," 2016.

[10] A. Cervone, A. Chierici, L. Chirco, R. Da Vià, F. Franceschini, V. Giovacchini, and S. Manservisi, "Development and Validation of Codes for the Coupling of the OpenFoam-Salome-FemLcore-Cathare Sofware for the Study of 4th Generation Lead-cooled Fast Reactors. Validation of the coupling with data experiments from the TALL-3D facility (Pt 1)," 2018.

[11] A. Cervone, A. Chierici, L. Chirco, R. Da Vià, F. Franceschini, V. Giovacchini, and S. Manservisi, "Development and Validation of Codes for the Coupling of the OpenFoam-Salome-FemLcore-Cathare Sofware for the Study of 4th Generation Lead-cooled Fast Reactors. Validation of the coupling with data experiments from the TALL-3D facility (Pt 2)," 2019.

[12] A. Cervone, L. Chirco, R. Da Vià, and S. Manservisi, "Development and validation of the FEMLCORE-SALOME-CATHARE coupling model of the TALL-3D facility with turbulence models," 2017.